Permeability Effect on the capillary and the viscous forces during the drainage process in porous media

CHAKIB SELADJI
Département de Génie Mécanique
Université Abou Bekr BELKAID
BP 119 Chétouane Tlemcen 13000
ALGERIA
seladji@yahoo.fr

Abstract: Two-phase flow and capillarity phenomenon in porous solids are well known in physics and engineering. In different studies, drainage experiments in porous media, initially saturated with a wetting fluid, have been largely devoted by using various type of fluids and different angle values of slant to the horizontal direction, in order to evaluate the effects of gravity forces and the injection flow-rate. However, the influence of the matrix structure on the capillary and viscous forces as well as the fluids distribution has not been treated sufficiently. In this study, we simulate an ascending air phase flow in a vertical porous channel initially saturated with a liquid phase, in order to evaluate the two previous effects. The numerical study is performed for large range of injected air mass flow rate along the porous channel from the bottom up. The different forces intervening in the drainage process is analyzed according to several permeabilities. The results show that for a weak gas mass flow rate, the capillary effect is dominant and the gas saturation in a porous channel is proportional to the permeability. For more important gas mass flow rate, the saturation behavior becomes inversely proportional to the permeability of the porous channel.

Key-Words: two-phase flow, capillary pressure, viscosity forces, relative permeability, saturation behavior

1 Introduction

Two-phase flows in porous media are phenomena currently met in various industrial fields. Examples include oil reservoir engineering, post accident analysis of nuclear reactors, drying processes and geothermal systems. In the oil industry, the primary petroleum recuperation covers only 30 to 40 percents of oil from oil fields. However, when oil production declines, a gas phase such as CO_2 is injected into the reservoir to mobilize the oil and increase the production. A large number of factors can affect this phenomenon, including capillary, viscous and gravity forces.

Many experiments were carried out in order to understand the dynamic and the invasion process [1], [2], [3]. Meanwhile, many analytical and numerical studies were developed in order to simulate different cases of capillary and gravity effects [4], [5]. Drainage studies have been largely devoted by using various types of fluids and different angle values. The porous medium will be subjected to pressure gradients due to the effects of gravity [6] and viscous forces [7], [8].

In this study, Hassler's experiments [9] are analyzed in order to compare the effects of the different forces intervening in a drainage process. These experiments consist of injecting from bottom up of a porous channel a non-wetting phase (gas).The top extremity is maintained wet using a reservoir of water. The porous matrix is saturated with the wet phase (water). A large range of a gas mass flow rate is applied to different permeabilities of porous channel.

2 Problem Formulation

Several mathematical models have been developed in order to describe two-phase flow in porous media. Bowen [10] developed a number of classical multi-component mixture models of two or several constituents, considering the average thermo-physical properties of the fluids. Using this homogeneous equilibrium flow model, the mixture is treated by the familiar single phase flow methods. The two phases are assumed to be intimately mixed and to have equal velocities and temperatures. Contrarily to the previous model, the separate flow model (SFM) given by Scheidegger [11], which uses every phase characteristics separately and takes into account the interactions between the fluids (the capillary pressure and the relative permeability), has been generalized by Grosser and al.[12] while

including the inertial terms. In fact, he demonstrated that for important velocities, these terms cannot be disregarded. It is clear that this model is more precise. However, it presents many difficulties that need to be solved. Some researchers, as Wang and Beckermann [13] built a two-phase mixture approach from a separate flow model. They introduced capillary effects and the relative permeability concept for small velocities. This consideration allowed them to disregard the inertial terms while using the linear formulation (Darcy's flow).

Our problem will be described using the Separate flow approach. The Darcy's law which governs the fluid flow in porous media was generalized for two-phase flow, including the macroscopic inertial terms for a steady state as follows: (for i =liquid, gas)

$$\frac{\rho_i}{\varepsilon.s_i}\cdot\left(\vec{v}_i.\nabla\vec{v}_i\right)=-\vec{\nabla}P^i+\rho_i\cdot\vec{g}-\frac{\mu_i}{K_i}\cdot\vec{v}_i+\frac{\mu_i}{\varepsilon\cdot s_i}\cdot\nabla^2\vec{v}_i \quad (1)$$

K_i and ε are respectively the effective permeability and the porosity of the porous medium. Note that (for i = liquid, gas):

$$K_i = K.K_{ri} \quad (2)$$

and K_{ri} are the relative permeabilities for each phase.

2.1 The relative permeability model

The relative permeability concept is introduced to describe the multiphase flows in porous media. Several studies were conducted to establish the relationship between the relative permeability for each phase and the saturation. The Van Genuchten–Mualem two-phase characteristic curves and Brooks-Corey correlation [14] are the most commonly used relationships. Many authors [15] use the Corey model (i.e.) power law functions to describe the relative permeabilities as follows:

$$K_{rl} = S_e^4 \quad (3)$$

$$K_{rg} = (1-S_e)^2(1-S_e^2) \quad (4)$$

In these equations, S_e is the effective liquid phase saturation defined by:

$$S_e = \frac{S_l - S_r}{1-S_r} \quad (5)$$

As given by Kaviany [16], the factors that could influence the relative permeability are the local saturation, the matrix (or pore) structure, the contact angle, the surface tension, and the density ratio. Effects of these factors are generally examined experimentally. Some empirical correlations are reported by Kaviany [16]. (see Table 1).

2.2 The Capillary pressure models

In this section, we will give a summary of the most important works related to the capillary pressure. Webb [14], mentions that the van Genuchten curves are the most widely used set of two-phase characteristic curves. The capillary pressure relationship is given by:

$$P_c = \frac{1}{\alpha}\left[S_e^{-1/m}-1\right]^{1/n} \quad (6)$$

Where α is the capillary pressure parameter, m and n are fitting parameters given from experimental data. These parameters are discussed by many authors and they proposed many correlations [14, 17,18].

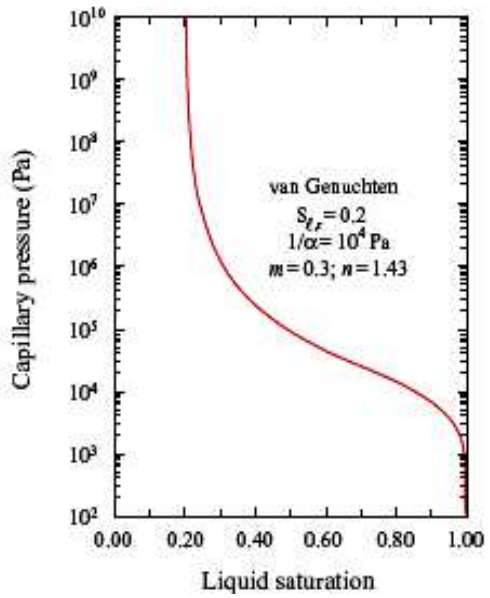

Fig.1 Representative van Genuchten–Mualem two-phase capillary pressure given from [14]

Webb [14] mentions that Brooks and Corey model is another popular set of two-phase characteristic curves. Based on experimental observations, the effective saturation is a linear function of capillary pressure on a log-log plot, or:

$$P_c = \frac{P_b}{s_e^{1/\lambda^*}} \qquad \text{for} \quad P_c \geq P_b \quad (7)$$

Where P_b and λ are respectively the bubbling pressure and the pore-size index. The bubbling pressure, which is also called the displacement

pressure, is the extrapolated capillary pressure at full liquid saturation.

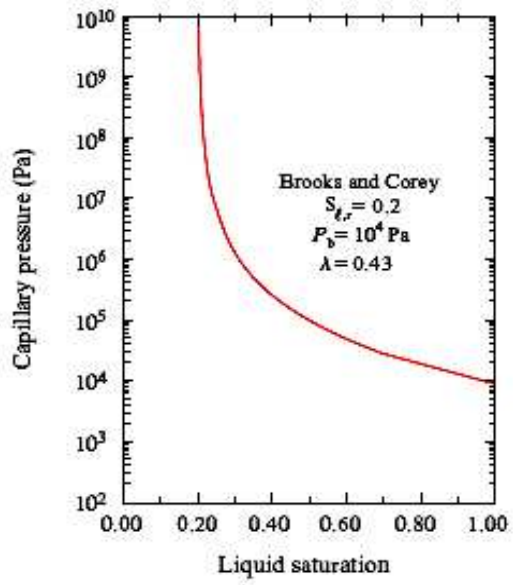

Fig.2 Representative Brooks and Corey two-phase capillary pressure given from [14]

While the van Genuchten and Brooks and Corey two-phase characteristic curves may look similar, there are important differences when they are used in flow situations. Webb [14] evaluated the differences between the two sets of characteristic curves for analytical two-phase flow situations. The differences in the saturation profiles are significant, probably due to the different shape of the gas-phase relative permeability expressions. In general, the van Genuchten set of curves lead to a much sharper interface, while the Brooks and Corey predictions are much blunter. On the other hand, Levrett as given by Kaviany [16] developed a correlation for capillary pressures in packed beds of unconsolidated materials:

$$P_c = \sigma \sqrt{\frac{\varepsilon}{K}} J(S_l) \tag{8}$$

$J(S_l)$ is the Levrett function which depends only on the liquid saturation S_l. σ is the surface tension between phases, ε is the porosity of the porous environment and K is the medium permeability.

Since, a general theoretical prediction of the capillary pressure is not obtainable, correlations are obtained from experiments. Table 2. gives several correlations used in the study of isothermal and iso-concentration two-phase flow in porous media. The correlations are made either to the imbibition or the drainage experimental data. Levrett function is generally used [16].

In order to take into account the variability of the capillary pressure according to permeability, the model of Scheidegger is used. This model presented in the equation (17), shows the relation between the capillary pressure and the saturation.

Table 1. Correlations for relative permeability [16]

Constraints	Correlation
(a) Sandstone and limestone, oil-water	$K_{rl} = S_l^4 \qquad K_{rg} = (1-S_l)^2(1-S_l^2)$ (9)
(b) Non-consolidated sand, well sorted	$K_{rl} = S_l^3 \qquad K_{rg} = (1- S_l)^3$ (10)
(c) Non-consolidated sand, poorly sorted	$K_{rl} = S_l^{3.5} \qquad K_{rg} = (1-S_l)^2(1-S_l^{1.5})$ (11)
(d) Connected sand stone, limestone, rocks	$K_{rl} = S_l^4 \qquad K_{rg} = (1-S_l)^2(1-S_l^2)$ (12)
(e) Sandstone oil-water	$K_{rl} = S_l^3 \qquad K_{rg} = 1 - 1.11.S_l$ (13)
(f) Soil water-gas	$K_{rg} = (1 - S_{ir} - S_{irg} - S_l)^{1/2}\left\{(1 - S_l^{1/m})^m - \left[1 - (1 - S_{ir} - S_{irg})^{1/m}\right]^m\right\}^2$ Where m is found experimentally (14)
(g) Glass spheres water-water vapor	$K_{rl} = S_l^3$ $K_{rg} = 1.2984 - 1.9832.S_l + 0.7432.S_l^2$ (15)
(h) sand water-air	$K_{rl} = \left(\frac{s_l - s_{lc}}{1 - s_{lc}}\right)^4 = \left(\frac{0.8 - s_g}{0.8}\right)^4$ $K_{rg} = \frac{25}{9}\cdot(s_g - 0.2)^2 \quad , \quad 0.2 \le s_g \le 0.65$ $K_{rg} = 1 - \frac{25}{7}\cdot(s_g - 1)^2 \quad , \quad 0.65 \le s_g \le 1$ (16)

(a) Corey reported by Wyllie (1962), (b-d) Wyllie (1962), (e) Scheidegger 1974 (p225), (f) Mualem 1976 reported by Delshad et Pope (1989), (g) Verma et Al. (1984) ,(h) reported by Houpert (1974)

Table 2. Different correlations for the capillary pressure given by Kaviany [16]

Constraintes	Correlations
(a) Water-air-sand	$\langle P_c \rangle = \frac{\sigma}{(k/\varepsilon)^{1/2}}\cdot\left[0.364\cdot\left(1 - e^{-40.(1-s)}\right) + 0.221(1-s) + \frac{0.005}{s - 0.08}\right]$ (17)
(b) Water-air-soil and sandstone	$s = s_{ir} + \frac{1 - s_{ir} - s_{irg}}{\left[1 + \left(a_1 \cdot \frac{\langle P_c \rangle}{\rho_l g}\right)^n\right]^{1-1/n}}$ (18)
(c) Imbibition Non consolidated sand (from Levrett data)	$\langle P_c \rangle = \frac{\sigma}{(k/\varepsilon)^{1/2}}\cdot\left[01.417\cdot(1 - s_e) - 2.120(1-s_e)^2 + 1.263(1-s_e)^3\right]$ $where \quad s_e = \frac{s - s_{ir}}{1 - s_{ir} - s_{irg}}$ where n > 1, a_1 is a constant given from experiments (19)
(d) Drainage, oil-water in sandstone	$\langle P_c \rangle = \frac{\sigma}{(k/\varepsilon)^{1/2}}\cdot\left[a_1 - a_2 \ln(s - s_{ir})\right]$ $a_1 = 0.30 \qquad a_2 = 0.0633 \qquad s_{ir} = 0.15$ (20)

(a) Scheidegger (1974) from Levrett experiments (1941), (b)Van Genuchten (1980), (c) Udell (1985), (d) Pavone (1989)

2.3 Boundary Conditions

2.3.1 Conditions on velocities

Let's consider $\vec{v}$ (u, v) in a Cartesian reference. U_{ie} is the velocity imposed at the entry (see Fig.3).
For ($i = l, g$)

$$\begin{cases} u_i\,(x,\, y=0) = 0 \quad , \quad v_i(x,\, y=0) = 0 \\ u_i\,(x,\, y=d) = 0 \quad , \quad v_i\,(x,\, y=d) = 0 \\ u_i\,(x=0,\, y) = U_{ie} \quad , \quad v_i\,(x=0,\, y) = 0 \\ \left.\dfrac{\partial u_i}{\partial x}\right|_{x=L} = 0 \quad , \quad v_i(x=L,y)=0 \end{cases} \tag{21}$$

2.3.2 Conditions on gas saturation

To be able to utilize information from known conditions, we consider that the area at the outlet of the porous massif to be wet at all time. This assumption permits to consider a critical gas saturation $S_{gc}=0.2$ as given by Houpert [4].

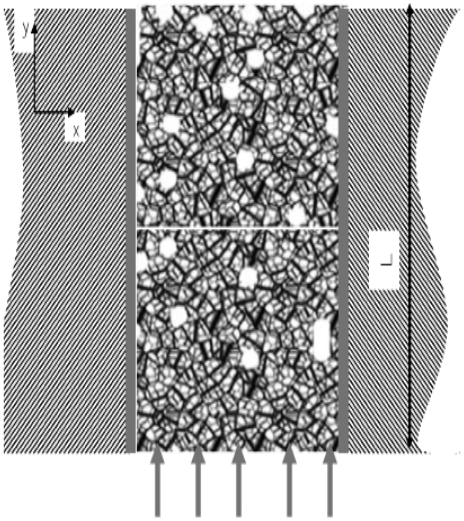

Fig. 3 Problem setting

3 Method of resolution

The problem is solved using the numerical finite volume method with a structured mesh and a finer grid at the exit side. The Semi Implicit Method for Pressure Linking Equation developed by Patankar [19] is used for the calculation of the pressure fields. The saturation S is known by identifying the pressure difference $P^g - P^l$ with the capillary pressure $P_c(S)$ represented by equation (17).

4 Results analysis

4.1 Test case

In order to validate our calculation code, the numerical solution [5] is compared with the analytical solution given by Houpert [4]. This analytical solution is given for a darcian flow (while omitting Brinkman and Forchheimer terms). In his calculation, Houpert used the formula in (22) and (23) related to the relative permeability and the capillary pressure:

$$P_c = \frac{64}{0.8 - s_g} \text{ (mbar)} \tag{22}$$

The capillary pressure model is given for a porous media with the following characteristics: ε = 0.2 and K = 2.10^{-13} m²

$$\left.\begin{aligned} K_{rl} &= \left(\frac{s_l - s_{lc}}{1 - s_{lc}}\right)^4 = \left(\frac{0.8 - s_g}{0.8}\right)^4 \\ K_{rg} &= \frac{25}{9}\cdot(s_g - 0.2)^2 \quad , \quad 0.2 \le s_g \le 0.65 \\ K_{rg} &= 1 - \frac{25}{7}\cdot(s_g - 1)^2 \quad , \quad 0.65 \le s_g \le 1 \end{aligned}\right\} \tag{23}$$

Fig.4 represents saturation profiles for different gas mass flow rates. From fig.5, we can note an increasing capillary pressure. It permits to deduce that it is necessary to exert an increasing gas injection pressure in order to obtain an increasing flow rate. In this case, gas saturation S_g increases fig.4. Identical results are given for an analytical solution of Darcy's linear equations for one-dimensional problems as given by Houpert [4].

A second test case is given. In this case, the analysis is undertaken while increasing the length of the porous channel. We impose the injected gas mass flow rate in the matrix initially saturated with water. The same boundary conditions are applied. Fig.6 shows that the gas saturation increases according to the channel length. The explanation is given from the pressure of gas injection, which increases with the length of the channel. In order to thwart the resistance of the porous environment to the flow, it is necessary to generate more important pressures. Therefore, the capillary pressure, which is the difference between the pressures of the two phases increase (see fig.7).

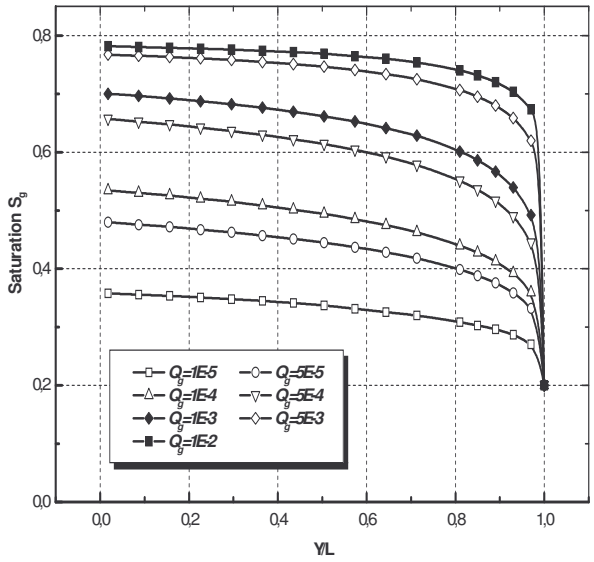

Fig. 4 Profile for the saturation for different mass flow rate

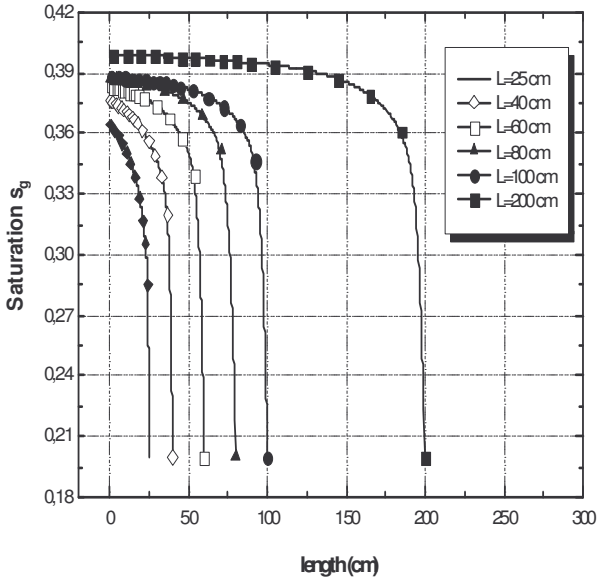

Fig. 6 Influence of the channel length one the liquid pressure injection

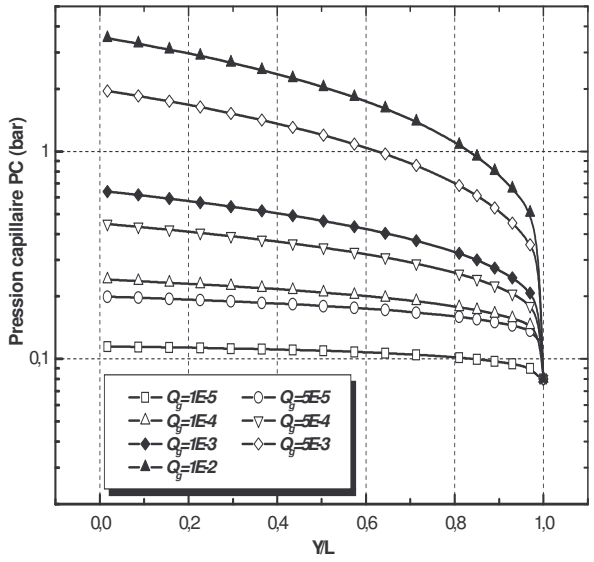

Fig. 5 Profile for the capillary pressure for different mass flow rate

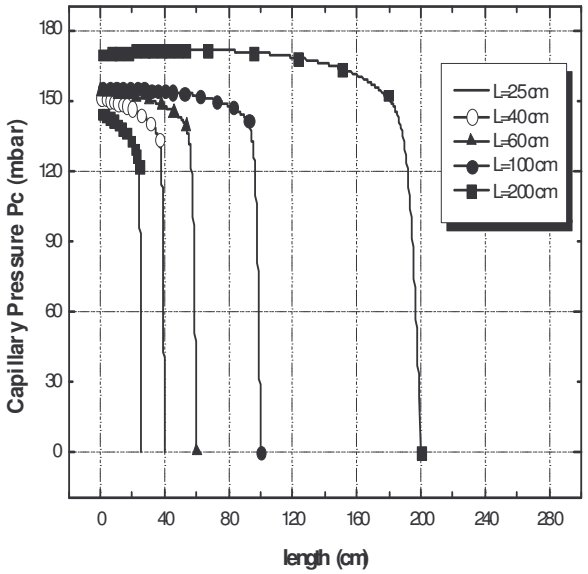

Fig. 7 Influence of the channel length on the liquid pressure injection

Q_g (kg/m².s)	10^{-5}	5.10^{-5}	10^{-4}	$5.\ 10^{-4}$	10^{-3}	$5.\ 10^{-3}$	10^{-2}
P_g (10^{-3} bar) Houpert (1974)	148.4	182.3	205.3	321.1	417.0	997	1639
P_g (10^{-3} bar) (current study)	145.9	178.5	202.8	318.4	415.1	991.3	1625.6
error %	1.7	2	1.2	0.8	0.4	0.5	0.8

Table 3. Comparison of the analytical results of the gas Pressure required at the injection with our numerical results for different gas mass flow rates

Table 3 shows a comparison of the analytical results [4] of the gas pressure required at the injection with our numerical results for different mass flow rates. The margin of error does not exceed 2%

4.2 Analysis of the capillary and viscous effects

The analysis of the capillary and viscous forces effects is proceeded using the relation (3) and (4) for the relative permeability and the relation (17) for the capillary pressure. In order to understand the behavior of the capillary pressure model, and to be able to interpret the two-phase flow thereafter, refer to fig.6, which shows the capillary evolution according to different porous channel permeability, while keeping a fixed porosity ε =0.2.

The graph shows that the capillary pressure behaves in an inverse way to the permeability. Moreover, we observe that for a same value of the S_g saturation, the capillary pressure decreases globally when the permeability increases. Therefore, for a same value of the capillary pressure, the saturation in gas becomes more important when the permeability increases. As a conclusion it would seem that a porous environment with an increasing permeability, submitted to the only capillary forces (slow flow), expands the saturation of the gas phase.

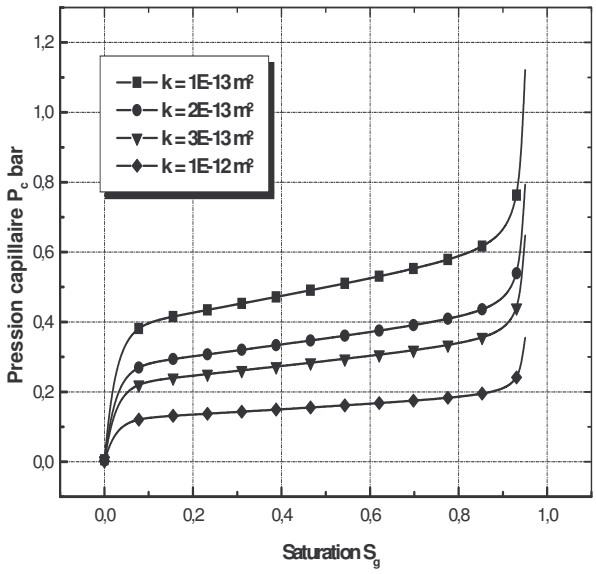

Fig. 8 The Behavior of Scheidegger capillary pressure model according to k, (ε =0.2)

In order to verify this hypothesis, we will proceed to simulations of gas flows in an initially saturated matrix with water. Two air mass flow rate will be examined, corresponding to a very slow flow (u_g=0,01 cm/s) and the other 100 times more important (u_g = 1 cm/s). The analysis of the two simulations permits to evaluate the influence of capillarity forces on the saturation in the different cases of permeability of the channel.

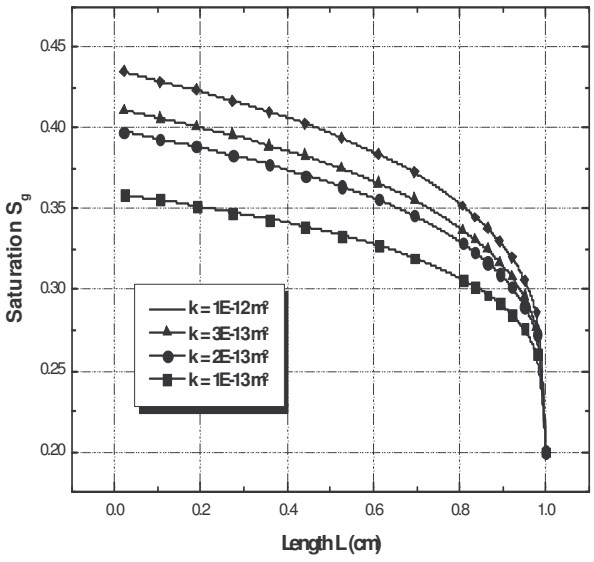

Fig. 9 The gas saturation behavior according to different k ($u_g=10^{-4}$ m/s)

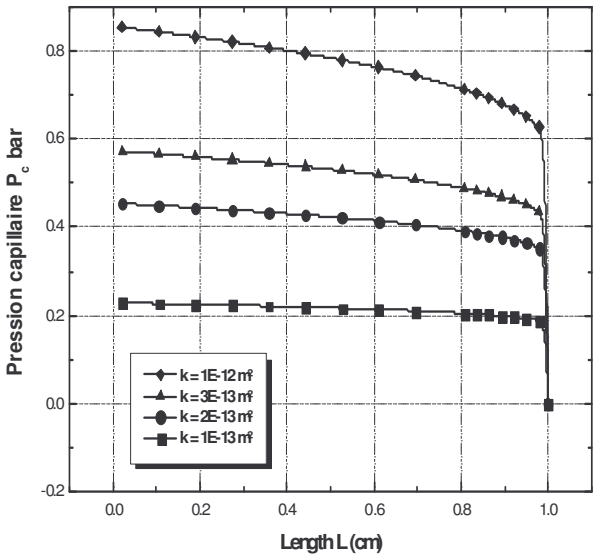

Fig. 10 The capillary pressure behavior according to different k ($u_g=10^{-4}$ m/s)

Fig.9, fig.10 describe respectively the gas phase and the capillary pressure behaviors within the porous massif for $u_g = 10^{-4}$ m/s (very slow flow). From the bottom to the top, the gas saturation decreases as well as the capillary pressure. At the exit side, the saturation corresponds to the boundary condition $s_g = 0.2$.

Following what has been stated previously, the saturation in a gas phase grows proportionally with the permeability k of the solid environment. This result needs, in order to be explained, an important number of analyses.

For more important velocities ($u_g = 10^{-2}$ m/s), we can conclude from fig.11 and fig.12 that the saturation in gas phase decreases for the increasing values of the permeability. This result announces an inverse behavior compared to the slow flows [20].

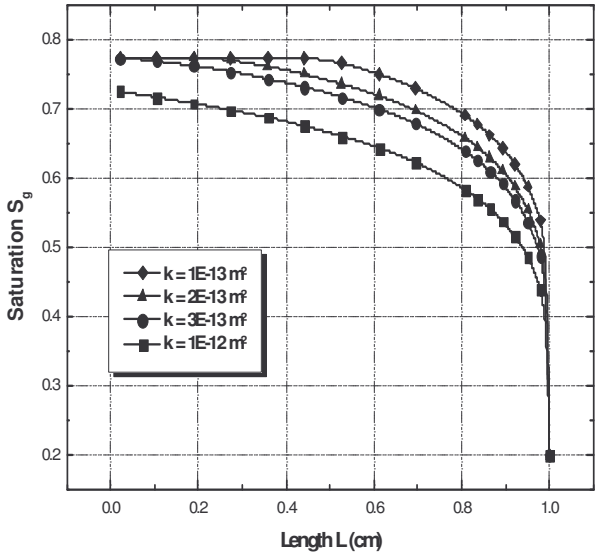

Fig. 11 The gas saturation behavior according to different k ($u_g=10^{-2}$ m/s)

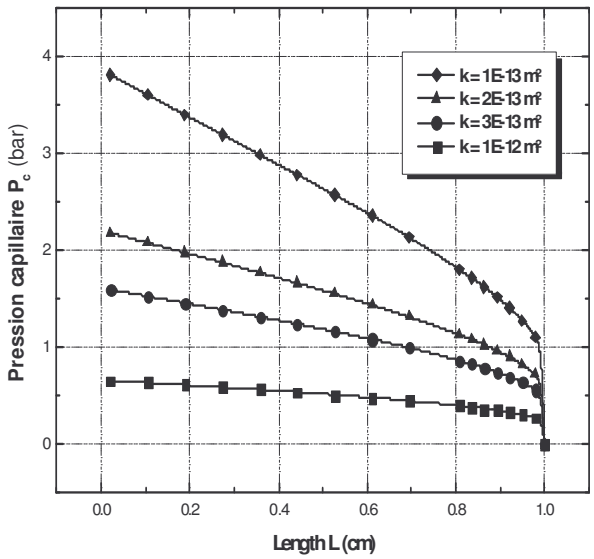

Fig. 12 The capillary pressure behavior according to different k ($u_g=10^{-2}$ m/s)

4-3 Discussion and Interpretation

In the governing equation, the capillary forces are represented by the capillary pressure model given by the relation (17). On the other hand, the difference between pressures in each phase can be represented by the following term:

$$\Delta P = \left| \left(\Delta\rho \cdot g - \frac{\mu_g}{K_g} \cdot u_g \right) . L \right| \qquad (24)$$

In the relation (24), the inertial effects are disregarded as well as a Brinkman term. We recall that the liquid phase has velocity $u_l = 0$. In order to quantify the importance of each term, we develop a comparative study between the capillary pressure model and the relation (24) is done. We can see for the first case (u_g=10 $^{-4}$ m/s), in fig.13, that for any gas saturation different from the residual value (s_g =0.2), the capillary forces are more important than the viscous forces, excluding the irreducible saturation value.For (u_g=10 $^{-2}$ m/s), we can conclude from the fig.14 that the viscous force becomes predominate. Its value increases when the permeability decreases.

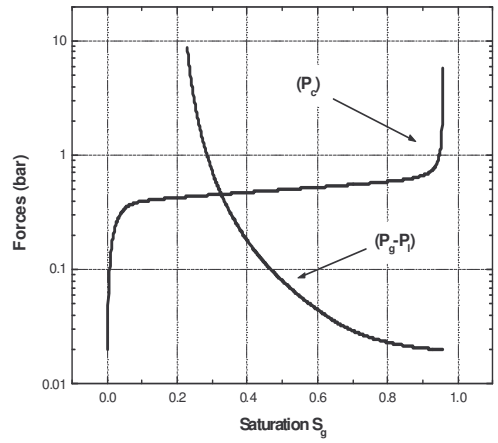

(a) $k = 10^{-13}\, m^2$

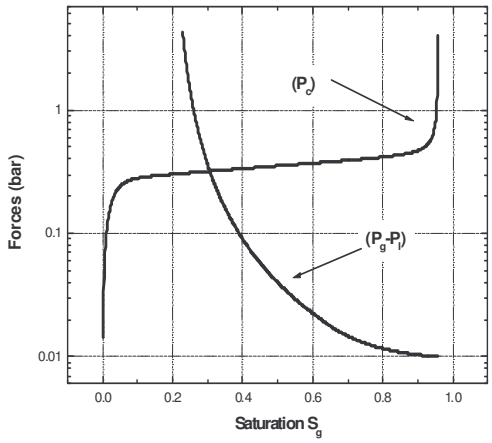

(b) $k = 2.10^{-13}\, m^2$

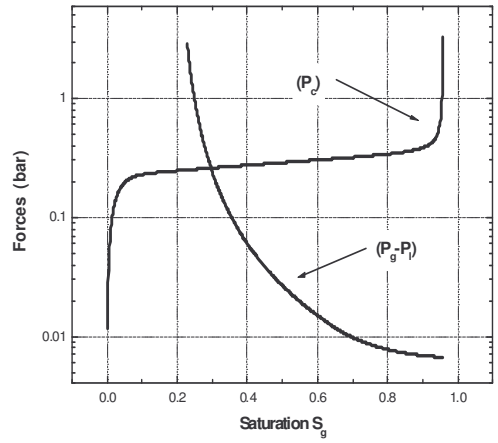

(c) $k = 3.\ 10^{-13}\, m^2$

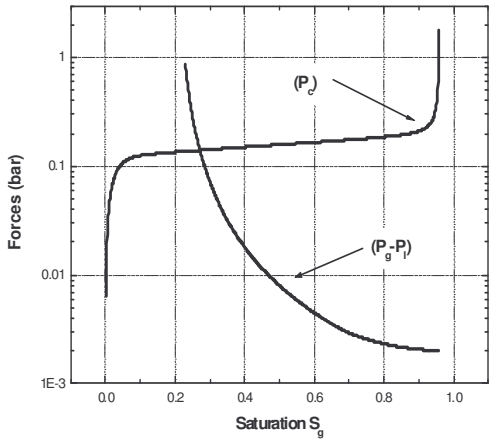

(d) $k = 10^{-12}\, m^2$

Fig. 13 Comparison between the viscous term and the capillary forces for different permeabilities (u_g=10 $^{-4}$ m/s)

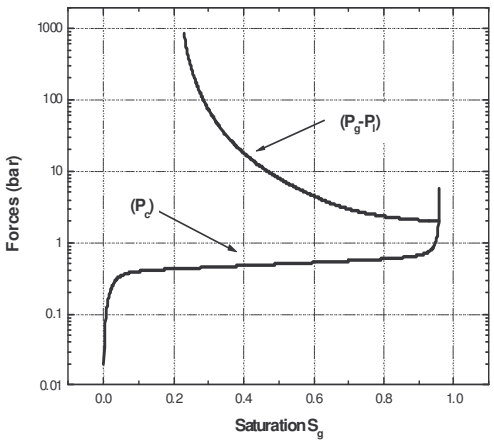

(a) $k = 10^{-13}\ m^2$

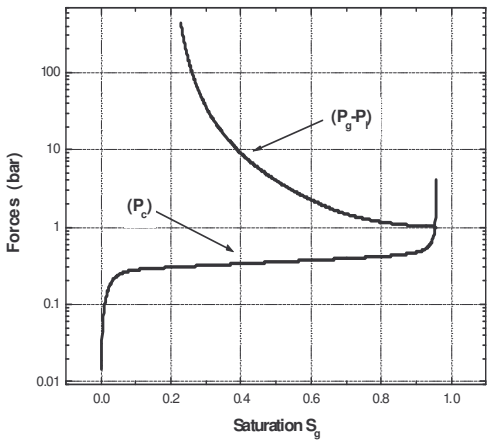

(b) $k = 2.10^{-13}\ m^2$

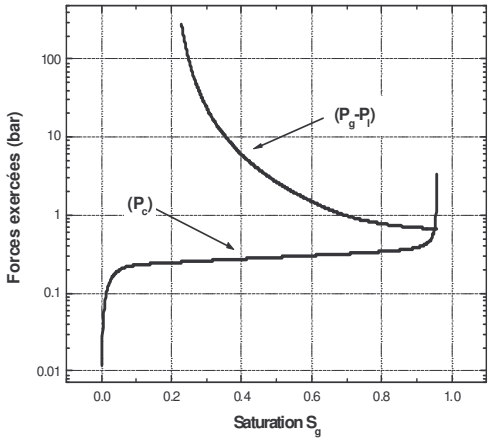

(c) $k = 3.10^{-13}\ m^2$

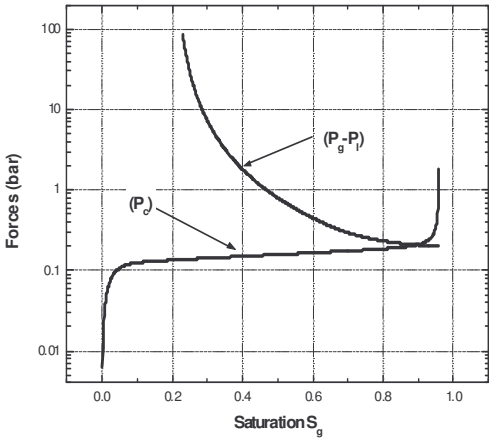

(d) $k = 10^{-12}\ m^2$

Fig. 14 Comparison between the viscous term and the capillary forces for different permeabilities (u_g=10 $^{-2}$ m/s)

4.3 Analysis of the effect velocities on capillary and viscous forces

In the previous section we have demonstrated that the gas saturation can have two distinct outcomes with regard to the permeability. We have applied two mass flow rate of gas corresponding to $u_g=10^{-4}$ m/s to $u_g=5.10^{-2}$ m/s. In order to give more details about the influence of the gas mass flow rate at different forces, a large range of velocities are applied.

We can see from the fig.15 that the viscous forces are proportional to the gas velocity. From $u_g=10^{-4}$ m/s to $u_g=10^{-3}$ m/s, the capillary forces are more important than the viscous forces excepted for the critical value of the saturation s_g = 0.2. The viscous forces become more important for more important values of velocities.

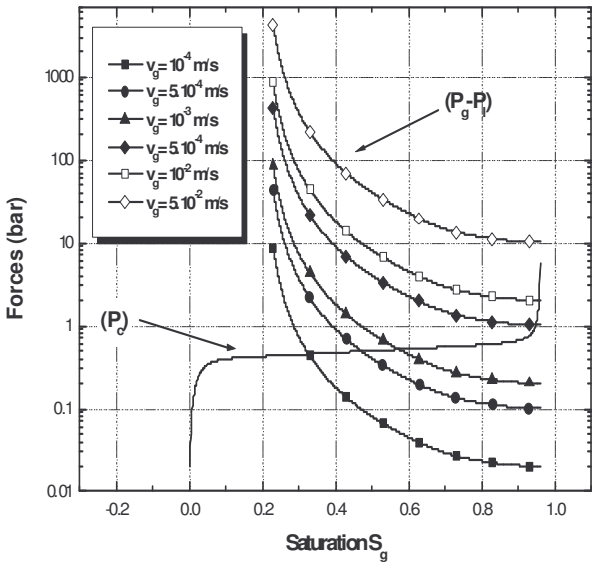

Fig.15 viscous term behavior for different gas mass flow rate ($K=10^{-13}$ m²)

On the other hand, we can see from the fig.16 that the saturation behavior comes closer when the permeability increase if we compare the two cases $u_g=10^{-4}$ m/s and $u_g=10^{-2}$ m/s. From this analysis, it seems that for an ideal permeability, we can obtain an optimum saturation of gas with a minimal value of the gas mass flow rate.

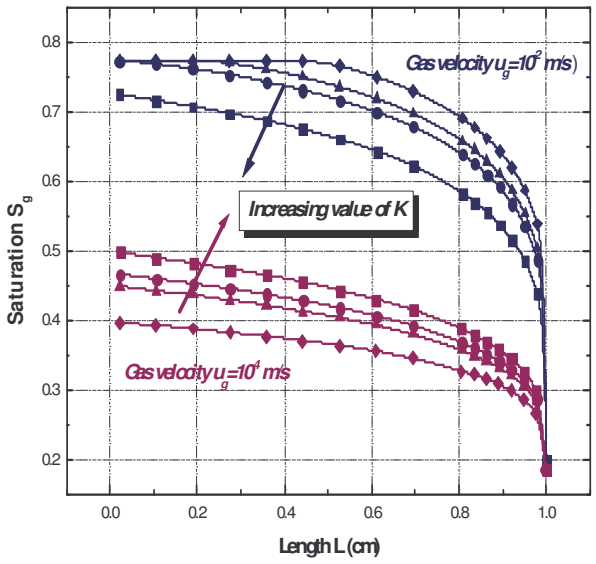

Fig. 16 comparisons of the gas saturation behaviors for an increasing value of permeability (high and low velocities cases)

5 Conclusion

In this study, we analysed the behavior of the injected gas saturation in initially saturated porous channel. The distribution of the gas phase is intimately related to the pressure drop. In general, we conclude that the saturation of the gas phase in the drainage process is influenced by the gas mass flow rate and the porous environment. This requires a sufficient pressure. However, a more meticulous analysis demonstrates that the distribution of gas phase behaves in two distinct ways next of the permeability. In the case of very slow flows, the saturation in gas phase is proportional to the permeability of the porous environment. The truly motor of the flow in this case is capillarity. In the case of faster flows, the saturation becomes inversely proportional to the permeability. The viscous forces become more important for weaker permeabilities.

Finally, we noted that for an increasing value of the permeability, the saturation behaviour comes closer for the two cases: high and low velocities. As a general conclusion, we expect that for an ideal value of the permeability, admissible by capillary pressure model, it's possible to find a minimal value of the gas mass flow rate corresponding to an optimal drainage process.

This result will be examined experimentally in further works. The distribution of phases will be determined from CT image arrays generated by X-ray CT scanner. The core assembly will be mounted and secured on a stepper motor that allowed movement of the core in and out of the X-ray gantry. We will be able to take measurements along the core.

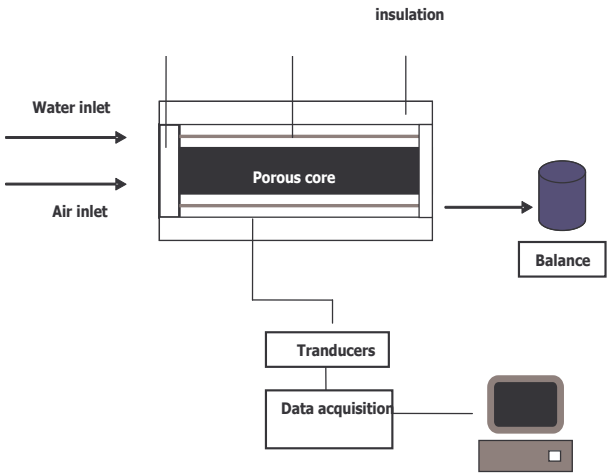

Fig.17 Experimental apparatus for the flow-through experiment

Actually, the Stanford Geothermal Program has conducted steam-water relative permeability experiments using the same apparatus. The major components of the experimental apparatus and the CT scanner are shown in fig. 17.

References:

[1] F.A.L. Dullien, Porous Media Fluid Transport and Pore Structure, *2nd ed. Academic, San Diego, 1992*

[2] J.Koplik, Creeping flow in two-dimensional networks, *J. Fluid Mech. 119, 1982, pp.219-247.*

[3] R. Lenormand, Déplacements polyphasiques en milieux poreux sous l'influence des forces capillaires – Etude expérimentale et modélisation de type percolation, *Thèse d'état I.N.P.T., Toulouse, France, 1981.*

[4] A. Houpert, Mécanique des fluides dans les milieux poreux critiques et recherches, *Technip edition, France 1974*, *pp.185 220.*

[5] C.Seladji, S. R. Taleb and Y. Khadraoui, Effect of gas phase flow on the flashing phenomena during an ascending two phase (liquid-gas) flow in a porous channel, *Journal of Porous media, Vol 10,N° 6 ,2007,PP. 525-536*

[6] Y.Meheust, G. Lovoll, K.J. Maloy, J. Schmittbuhl, Interface scaling in a two dimensional porous medium under combined viscous, gravity, and capillary effects. *Physical Review E 66, 0516011-0516031,* 2002.

[7] G. Lovoll, Meheust, Y., Toussaint, R., Schmittbuhl, J., Maloy, K. J., Growth activity during fingering in a porous Hele-Shaw cell. *Physical Review E 70, 263011-2630112, 2004.*

[8] P. Meakin, G. Wagner, A. Vedvik, H.K. Amundsen, J. Feder, T. Jossang, Invasion percolation and secondary migration: experiments and simulations. *Marine and Petroleum Geology 17, 2000, .pp.777-77.,*

[9] G. L. Hassler, R. R. Rice, and E. M. Leeman, Investigation on recovery of oil from sandstone by gas-drive. *Trans. AIME, 118, 1936, p. 116,*

[10] R. Bowen, Theory of mixture. *In continuum Physics III (Edited by A. C. Eringer). Academic press, New York, 1976*

[11] A.E. Scheidegger, The physics of flow through porous media, *third edition, university of Toronto press, 1974*

[12] K. Grosser, R. G. Carbonell, and S. Sundaresan, Onset of Pulsing in Two Phase Co-current Down Flow Through Packed Beds*, AIChE J., 34, pp. 1850-1860, 1988*

[13] C.Wang and Beckermann C., A two phase mixture model of liquid-gas flow and heat transfer in capillary porous media I-Formulation. *Int. J. Heat mass transfer vol.36, No.11, pp.2747-2758, 1993*

[14] C. K. Ho, S.W.Webb, Gas Transport in Porous Media, *Springer edition, 2006.*

[15] R.N Horne, C. Satik, G. Mahiya, K. Li, W. Ambusso, R.Tovar, C.Wang and H. Nassori, Steam-water relative permeabilty, *2000 World geothermal Congress, 2000, pp. 186-193.*

[16] M. Kaviany, Principals of heat transfer in porous media, *Mechanical engineering series, Springer edition, 1995*

[17] R.Van Genuchten, Calculating The Unsaturated Hydraulic Conductivity With a New Closed-Form Analytical Model, *Water Resources Bulletin 78-WR-08, Department of Civil Engineering, Princeton University, 1978*

[18] Y. Mualem, , A New Model for Predicting the Hydraulic Conductivity of Unsaturated Porous Media, *Water resources Research, Vol. 12, no. 3, 1976, pp. 513–522.*

[19] S.V. Patankar, Numerical heat transfer and fluid flow, *Mac Graw Hill, 1980*

[20] C. Seladji, Influence of the capillary and the viscous forces during the drainage process in a porous media, *proceeding of the 3rd WSEAS international conference on Applied and Theoretical Mechanics, Spain décembre2007, pp.202-205*